Marine Geology 497 (2026) 107792

Contents lists available at ScienceDirect

Marine Geology

journal homepage: www.elsevier.com/locate/margo

Research Article

Unveiling the origin of enigmatic seabed morphologies on the Cape Licosa ridge (Italy)

Valentina Alice Bracchi [a,b,*], Sara Innangi [c], Renato Tonielli [c], Gemma Aiello [c], Pietro Bazzicalupo [a], Daniela Basso [a,b], Davide Vernazzani [c], Valentina Grande [d]

[a] University of Milano-Bicocca, Department of Earth and Environmental Sciences - DISAT, Piazza della Scienza 4, 20126 Milano, Italy
[b] CONISMA - Consorzio Interuniversitario per le Scienze del Mare, Piazzale Flaminio 9, 00196 Roma, Italy
[c] National Research Council, Institute of Marine Science, Napoli local unit, Calata Porta di Massa, 80133 Napoli, Italy
[d] National Research Council, Institute of Marine Science, Bologna local unit, Via Piero Gobetti, 101, 40129 Bologna, Italy

ARTICLE INFO

Editor: Michele Rebesco

Keywords:
Submarine geomorphology
Cilento Flysch
Last Glacial Maximum
Paleo-topography
Holocene sedimentation
Mesophotic habitats

ABSTRACT

High-resolution marine geophysical surveys conducted in 2004 revealed submarine morphologies offshore Cape Licosa (Tyrrhenian Sea, Italy), whose origin remains debated for years. Remote and direct data collected within the CORSUB project between 2024 and 2025 identified a field of subcircular to polygonal mounded structures distributed between approximately 75 m and 90 m of water depth along a ridge. These bedforms were analyzed using multibeam bathymetry and backscatter data, side-scan sonar, sub-bottom profiling, and video observations. CHIRP profiles indicate that these morphologies occur above a rugged acoustic basement attributed to the Miocene Cilento Flysch, which is draped by a thin, discontinuous Holocene sedimentary cover. Morphometric analysis delineated 565 discrete features with average dimensions of 8.6 × 6.1 × 0.4 m and a prevailing northeast to southeast orientation. They exhibit a distinctive high-reflectivity ring surrounding a lower-reflectivity core, producing a regular beehive-like seabed texture. Videos document a wavy-profiled seascape characterized by coarse-grained biogenic sediments, including abundant boxwork rhodoliths, and localized encrustations of coralline algae and bivalves on rocky outcrops.

The data suggest that an inherited, complex paleo-topography of the Flysch substrate formed during subaerial exposure of the ridge at the Last Glacial Maximum. Holocene sedimentation draped this surface, involving both sediment accumulation driven by intense hydrodynamic activity and benthic colonization of sparse rocky substrates, thereby preserving this complexity and resulting in a wavy seafloor profile. These findings highlight the control of paleo-topography and post-glacial sedimentary dynamics in shaping mesophotic seabed morphology and distinctive seabed landforms along Mediterranean continental shelves.

1. Introduction

Recent advances in marine exploration, combined with the progressive refinement of remote and direct survey techniques, have revealed a wide range of unusual submarine morphologies that vary in form, size, and extent, and often remain enigmatic in both origin and nature. The formation of these bedforms is not always straightforward and can result from complex interactions among fluid seepage, submarine currents, sediment transport, biogenic accretion, glacial processes, and tectonic activity (e.g.: Parsons et al., 2019; Meredyk et al., 2020; Böttner et al., 2024; Aiello and Caccavale, 2025; Innangi et al., 2025). Their scientific importance lies in their value as indicators of poorly understood processes, whose correct interpretation may be crucial for resource and hazard management and for understanding the geological record.

In particular, the exploration of shelf environments, from coastal to offshore areas, has revealed the essential role of organogenous bioconstruction in characterizing seabed and seascape. This process involves developing complex mobile and stable structures that alter the seabed's physical properties over time (Harris, 2020), thereby

* Corresponding author.
E-mail addresses: valentina.bracchi@unimib.it (V.A. Bracchi), sara.innangi@cnr.it (S. Innangi), renato.tonielli@cnr.it (R. Tonielli), gemma.aiello@cnr.it (G. Aiello), pietro.bazzicalupo@unimib.it (P. Bazzicalupo), daniela.basso@unimib.it (D. Basso), davide.vernazzani@cnr.it (D. Vernazzani), valentina.grande@cnr.it (V. Grande).

https://doi.org/10.1016/j.margeo.2026.107792
Received 18 November 2025; Received in revised form 29 April 2026; Accepted 29 April 2026
Available online 5 May 2026

contributing to the formation and maintenance of unique habitats. These features are no longer simply sedimentary accumulations; they are accretions capable of influencing the morphological development of the shelf profile and the seascape through time.

Moreover, sea level variations associated with Pleistocene climatic phases modified the paleo-topography of the actual continental shelf and contributed in providing complex paleo-topography available for colonization by benthic organisms over time. This effect was particularly pronounced during the Last Glacial Maximum, when sea level dropped by 120 m (mean value) (Lambeck et al., 2004), exposing submerged coastal and offshore paleo-seascapes, that were markedly different from present conditions. This subsequentially influenced the shelf development during the Holocene (Micallef et al., 2013; Deiana et al., 2021). Biogenic activity often exploits such conditions and contributes to the formation of biogenic substrates in geomorphological settings shaped by recent seafloor modeling events (e.g., Varzi et al., 2023; Ximenes Neto et al., 2025).

Seafloor morphologies can now be studied using quantitative approaches which allow to better distinguish and characterize bedforms. Geomorphometry applies image-processing techniques to quantify the shape of Earth's topography across various spatial scales. It focuses on the calculation of surface parameters, which can improve the mapping and modeling of landforms, vegetation, land use, natural hazards, and other phenomena (Pike and Dikau, 1995; Pike et al., 2009) as well as revealing spatial patterns more effectively.

In 2004, a geophysical survey offshore Cape Licosa in the Tyrrhenian Sea (Cilento Promontory, Campania Region, Italy) documented previously unknown seabed morphologies. They were located at that time approximately between 80 and 100 m water depth (mwd), along a ridge, and they showed a beehive-like arrangement (Bracchi, 2006). Only side-scan sonar imagery was available, which revealed circular to hexagonal clusters of "cells" forming a regular geometric pattern on the seafloor, suggesting an organized and repetitive texture. The acoustic signal was interpreted as the combined response of mobile sediments and rigid seafloor. Limited grab sampling conducted in 2004 provided preliminary insights indicating the presence of boxwork rhodoliths on a detrital seafloor. This initial evidence led to the hypothesis of a biogenic origin of these bedforms (Bracchi, 2006), as reef-building organisms can form persistent and stable structures that sustain benthic ecosystems. While corals are generally the most widely recognized reef-builders, other organisms, including mollusks, bryozoans, sponges, and particularly crustose coralline algae can also play a significant role. This is particularly true for the Mediterranean Sea, where coralline algae are considered as the most effective biogenic reef engineers, capable of colonizing both euphotic and mesophotic settings (Ballesteros, 2006; Bracchi et al., 2017). In mesophotic environments, they generate both mobile rhodolith deposits and more stable seafloor structures, such as coralligenous reefs, including discrete pillars (Di Geronimo et al., 2002; Bracchi et al., 2017) and (kilometer-wide) biogenic banks (Bracchi et al., 2017). Moreover, coralline algae are known for their ability to develop distinctive geomorphological build-ups, such as the coralligenous atolls of Corsica (Bonacorsi et al., 2012), the mounds of the Marmara Sea (Aksu et al., 2018), and the table-to-spiral cones of Linosa (Innangi et al., 2025).

After 2004, despite several exploratory efforts offshore Cape Licosa (Ferraro et al., 1997; Pennetta et al., 2013; Savini et al., 2012; Grande et al., 2015; Martelli et al., 2016; Aiello, 2019; Aiello and Caccavale, 2021; Savini et al., 2021; Aiello and Caccavale, 2023, 2024, 2025), no further occurrences of these subcircular morphologies have been observed. The CORSUB (To the CORe of the SUBstrate: inception and development of Mediterranean algal reefs) project was developed to investigate the origin, evolution, and potential ecological significance of Cape Licosa bedforms by collecting and integrating geophysical, stratigraphic, sedimentological, and paleontological data. In this paper, we provide a geomorphological and morphometric description and characterization of these enigmatic features and an interpretation of their origin.

1.1. Geological setting

Punta Licosa Promontory (= Cape Licosa) corresponds to the northern boundary of the Cilento peninsula, between Castellabate Plain and Ogliastro Bay (Fig. 1a, b). The subaerial part of the promontory lies within the Cilento and Vallo di Diano National Park, while the submerged part is partially included in the Marine Protected Area of Santa Maria di Castellabate (Fig. 1b). The coastal landscape is dominated by siliciclastic units of the Cilento Flysch Group (Martelli et al., 2016), which form high cliffs (Valente et al., 2017), and by Quaternary units (Fig. 1b), composed of marine, transitional and alluvial sediment in angular unconformity on the siliciclastic turbiditic substrate, often associated with Middle to Late Pleistocene terraced surfaces (Aiello, 2019; Savini et al., 2021; Aiello and Caccavale, 2024).

Offshore, the continental margin is characterized by the seaward extension of the promontory. The seabed topography is complex. Seismic data revealed a deformed acoustic basement, displaced by Quaternary faults with sharp, steep scarps similar to those identified on land. The width of the continental shelf is variable, ranging from 30 km to the north of Punta Licosa (Trincardi and Field, 1991) to only 6 km to the south. Moreover, a series of submerged terraces, sculpted by Quaternary sea-level fluctuations and linked to both erosional and depositional processes have been identified in the area (De Pippo and Pennetta, 2000; Aiello, 2019; Savini et al., 2021; Aiello and Caccavale, 2024). The area experienced uplift until the Middle Pleistocene and has remained tectonically stable since then (Antonioli et al., 2004; Lambeck et al., 2011). Lambeck et al. (2004) reported that the sea level dropped to 140 m below present sea level during the Last Glacial Maximum, followed by a rapid rise that stabilized around 7500 kyrs BP.

Previous studies showed that the continental shelf stratigraphy comprises four seismo-stratigraphic units, often associated with shallow gas accumulations (Aiello and Caccavale, 2021). These units constitute the Quaternary basin in the study area and overlie the acoustic basement identified as Cilento Flysch accumulations (Aiello and Caccavale, 2021).

Present-day sedimentation along Cape Licosa includes toe-of-coastal-cliff deposits, submerged-beach deposits, inner- and outer-shelf deposits, low-stand system tract and Pleistocene relict marine units (Aiello and Caccavale, 2025). The littoral, inner shelf, and outer shelf environments have been interpreted as the high-stand system tract of the Late Quaternary depositional sequence (Aiello and Caccavale, 2025). Inner shelf deposits include fine- to coarse-grained sediment; *Posidonia* meadows (EMODnet Seabed Habitats product, 2023) and rhodolith beds (Savini et al., 2012). Outer shelf sediments include medium- to fine-grained sand with bio- and litho-clasts rich in rhizomes of marine phanerogams; as well as pelites. In addition, coralligenous formations occur on rocky substrates in the submerged portion of Cape Licosa (D'Angelo et al., 2020). Specifically, previous maps of the studied area (Fig. 1) classify the seabed as "Undifferentiated substrate - Silicoclastic and carbonate deposits, Tertiary" (D'Angelo et al., 2020).

1.2. Oceanographic setting

De Ruggiero et al. (2016, 2020) developed high-resolution models of water circulation along the Campania coastal system, reconstructing scenarios at 100, 200, and 500 mwd that include the studied area. The model indicates that circulation is strongly influenced by the interaction among wind forcing, topographic constraints, and the remote large-scale circulation in the Tyrrhenian Sea. In the study area, the 200 m depth scenario shows that currents flow southwesterly, with peak velocities up to 10 cm/s and seasonal variations in flow intensity.

2. Materials and methods

The study area corresponds to a ridge located offshore Cape Licosa

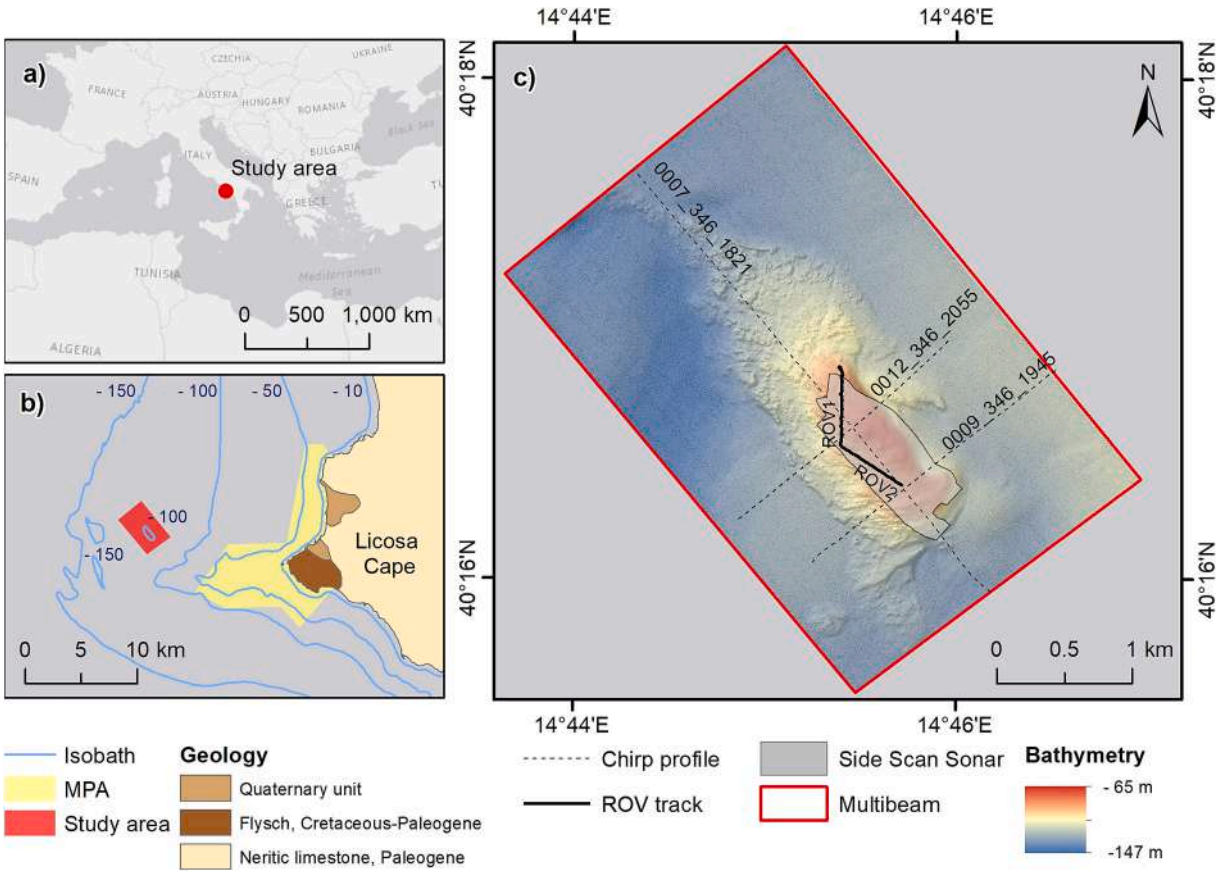

Fig. 1. a) Geographical and b) geological setting of the study area with the indication of the studied area (red box). b) reports the main geological units outcropping on land and along the coast of Cape Licosa. c) close-up of the study site which indicates the data collected for this paper: bathymetric surface (1 m resolution) on shaded relief (z factor = 5) (TREMOR) (red solid line), Chirp profiles (TREMOR), ROV tracks (CORSUB-2). Light-gray polygon indicates the area covered by Side Scan sonar data (CORSUB-1). Service Layer Credits: Esri, HERE, Garmin, © OpenStreetMap contributors, and the GIS user community. (For interpretation of the references to colour in this figure legend, the reader is referred to the web version of this article.)

(Tyrrhenian Sea, Italy) (Fig. 1c).

2.1. Data acquisition

High-resolution geophysical and geological data were collected within the framework of the CORSUB-1 (06/2024), TREMOR (12/2024), and CORSUB-2 (04/2025) oceanographic cruises (Fig. 1c).

The CORSUB-1 cruise was conducted aboard the catamaran motor vessel "Enviroconsult" operated by Enviroconsult S.r.l. to collect high-resolution backscatter data using the Klein System 3900 Side Scan Sonar (SSS). Approximately 0.70 km^2 of SSS data were acquired at depths ranging from 65 to 100 m, where the seabed features are present (Fig. 1c). The sonar was operated at an average altitude of approximately 20 m above the seabed, with a lateral swath set at 75 m to ensure high-resolution acquisition. During the TREMOR cruise, conducted aboard the research vessel Gaia Blu, owned by the National Research Council of Italy (Consiglio Nazionale delle Ricerche, CNR), morpho-bathymetric and stratigraphic data were collected. The morpho-bathymetric data were collected using a Kongsberg EM2040 high-resolution multibeam echosounder (MBES), capable of acquiring both bathymetry and backscatter data. The MBES was hull-mounted in a T-configuration of linear transducer arrays. A Seapath 380 system was used for ship positioning, supported by a Fugro HP differential Global Positioning System, with Marinestar GNSS signal accuracy better than 5 cm. The Kongsberg MRU motion sensor and a dual-antenna GPS integrated into the Seapath were used to correct for pitch, roll, heave, and yaw movements (Foglini et al., 2015). A 20% overlap between the bathymetric lines was mantained to ensure 100% bathymetric coverage of the entire study area. Stratigraphic data were collected using a Knudsen 3260 – CHIRP sonar profiler operating at 12 kHz and completed by nine 3.5 kHz transducers (Fig. 1c).

During the CORSUB-2 cruise, the Remotely Operated Vehicle (ROV) Perseo was used to acquire seafloor video footages across in the study area. Two linear transects were conducted (Fig. 1c). Transect ROV 1 (479,306.49 E, 4458958.73 N) was acquired in the western sector, along a bearing of 180°, covering a depth range of 90–94 mwd, and a length of approximately 600 m. Transect ROV 2 (479,312.55 E, 4458397.62 N) was acquired in the southern sector, along a bearing of 122°, covering depth range of 84–90 mwd, and a length of 570 m.

2.2. Geophysical data processing

Bathymetric data processing was conducted using QPS Qimera software (Quality Positioning Services BV, Zeist, Netherlands) following a standard procedure, that includes sound-speed correction, removal of erroneous soundings, and correction of vertical offsets from previous swaths. A light spline filter within Qimera was applied to remove soundings beyond the local mean water depth. Remaining offsets were removed manually using the Qimera "Slice Editor", to ensure data accuracy and preserve morphological structures. The processed bathymetric data were exported in GFS format for backscatter processing using the QPS Fledermaus Geocoder Tool (FMGT). The processed MBES data (.gfs) were used to apply backscatter corrections, beam pattern correction, and angle-varying gain corrections to the backscatter data. Following these corrections, FMGT applied the sonar's navigation data (i.e., XY coordinates, roll, heading, pitch, and heave) to georeference the

backscatter values. Finally, the backscatter lines were mosaicked using an algorithm designed to minimize blending between overlapping areas by 30–40%.

The final acoustic image was generated at 50 cm pixel resolution in gray-scale colour, with darker tones indicating higher reflectivity (Figs. 2, 3).

SSS data were processed using the latest release of *Seaview Mosaic* (Moga Software © Inc), which exploits modern computational capacity to preserve data at full resolution without the need for reduction. Geometric (slant range) and radiometric corrections were applied to each line, and a Beam Angle Compensation algorithm was used to equalize signal intensity along- and across-track while accounting for tow fish altitude variations. A de-striping procedure further removed artifacts associated with the tow fish roll motion. Advanced navigation processing tools were used to accurately reposition SSS lines, enabling precise adjustment of each ping without fanning. The final mosaic is a 20-cm-resolution acoustic image of the seafloor, generated by assembling grayscale SSS lines, where darker areas indicate higher reflectivity and lighter areas correspond to absorption or shadow zones beyond seafloor reliefs.

CHIRP data processing and interpretation were conducted using the GeoSuite AllWorks software package. This software enables the sequential application of various correction and enhancement algorithms, ensuring a clear, interpretable representation of the main stratigraphic discontinuities. Following this procedure, CHIRP data were converted subsequentially from raster to SEG-Y to JPEG format (Fig. 4).

2.3. ROV analysis

ROV videos were analyzed to identify substrate type (sediment or rock) and to document the presence of seafloor morphologies and benthic organisms, including build-ups and rhodoliths, with particular focus on the enigmatic seafloor structures (Fig. 5). Video frames corresponding to these morphologies were extracted using Avidemux 2.8.1 ([http://www.avidemux.org], last accessed on 23 September 2025).

2.4. Derivation of terrain attributes

The mathematical representation of the bathymetric surface through terrain and topographic variables enable geomorphological interpretation, and is also employed as a proxy in benthic habitat mapping, suitability modeling, and the assessment of ecological patterns (Lecours et al., 2016). In this study, topographic variables were generated to evaluate their potential for delineating specific seabed features. A set of terrain attributes (Table 1), derived from pixel-based analyses, and related to slope, curvature, and terrain variability was generated to support both manual and automatic pixel-based mapping. Using the Digital Elevation Model as a starting point, terrain attributes were calculated using GIS-based tools: the ArcGIS Spatial Analysis, the Benthic Terrain Modeler (NOAA) (Walbridge et al., 2018), and the Terrain Attribute Selection for Spatial Ecology (TASSE) Toolbox v. 1.1 (Lecours, 2017).

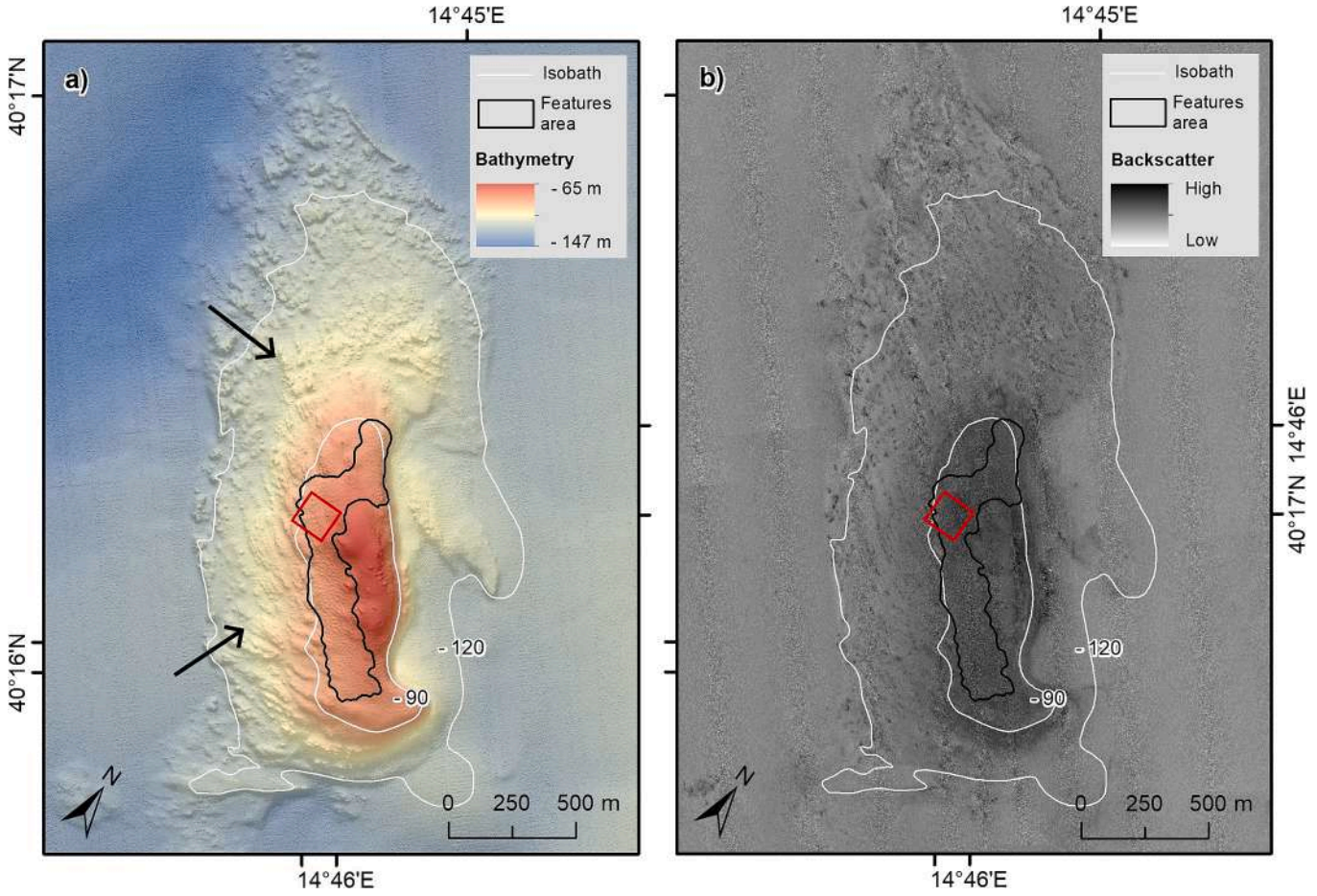

Fig. 2. MBES (a) and Backscatter (b) data of the studied ridge, with the indication of the −90 and − 130 contour lines. Black arrow indicates the zone where seafloor shows a complex topography. The area has been rotated of 35° with respect to the North. Black line contour indicates the zone where the studied features occur. Red boxes in a) and b) indicate the close-up in Fig. 3. (For interpretation of the references to colour in this figure legend, the reader is referred to the web version of this article.)

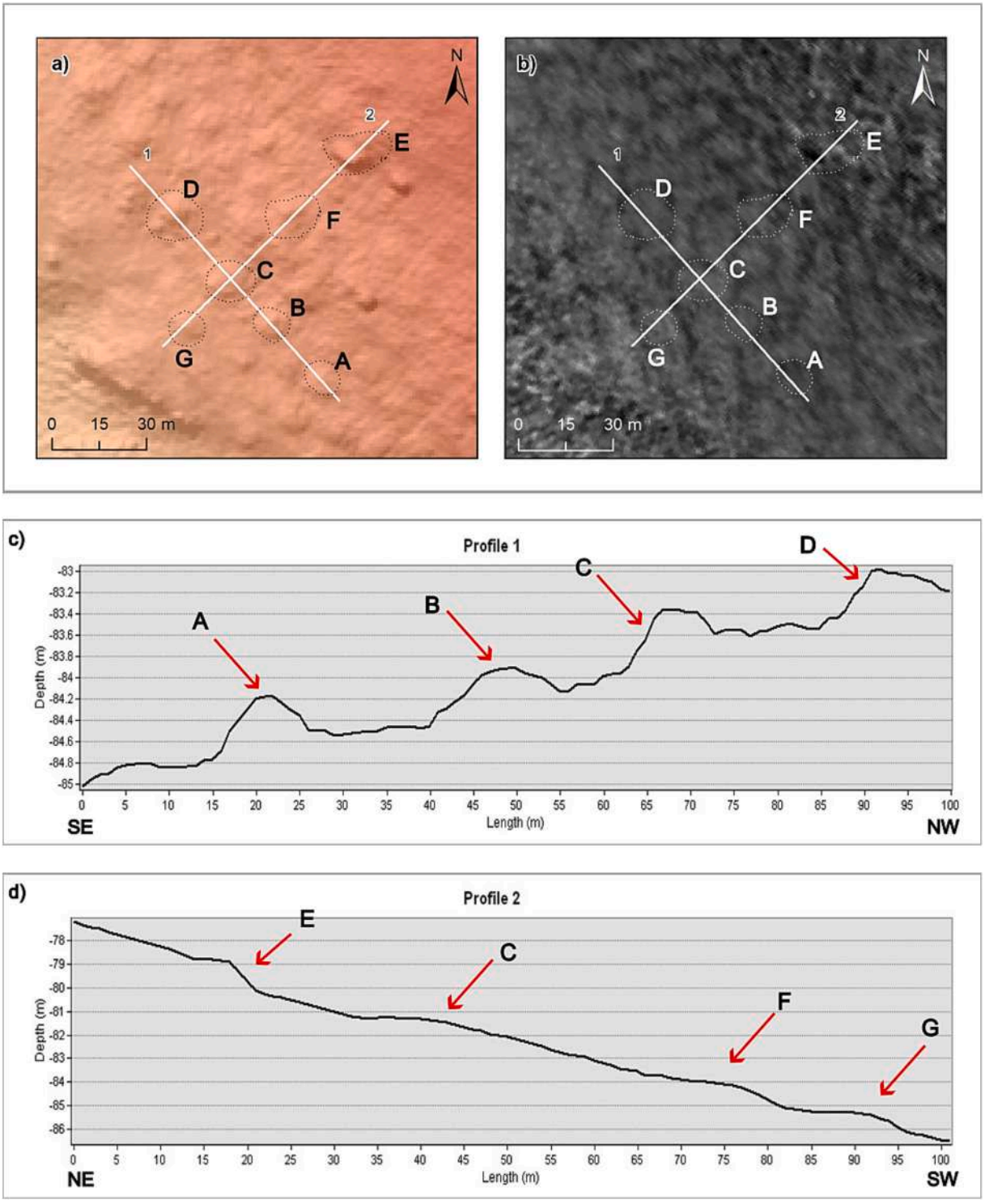

Fig. 3. Close-up on MBES (a) and backscatter (b) data of the area which included the bedforms studied in this paper, indicated by dotted black contours and capital letters. a) and b) correspond to the red box in Fig. 2. In b), the *beehive*-like patters is visible. Panels c) and d) show two topographic profiles. The track of the profile is indicated in a and b. c) Profile 1 shows that the bedforms may have conical (A and C), rounded (B) or squared (D) outlines. d) Profile 2 shows that, in orthogonal direction with respect to Profile 1, the bedforms are gently steep and with a wavy surface.

2.5. Delineation of seabed forms

To map the seabed forms targeted in this study, a semi-automatic process was employed using the Confined Morphologies Mapping (CoMMa) toolbox version 1.3 (Arosio et al., 2024) for ArcGIS Pro (© Esri) followed by expert manual supervision. The CoMMa Boundary-based delineation tool was used to delineate the seabed forms (positive features) from the raster obtained at the pre-processing stage using the CoMMa Local Topographic Position (LTP) tool. LTP metrics quantify how elevated or low-lying a site is relative to local topographic variability; providing a scale-dependent measure that varies according to the size of the neighboring area used for comparison (Lindsay et al., 2015). In this study, a mean-derived LTP metric was applied with a deviation from mean elevation (DEV) of 3.5. The Mean-DEV LTP raster

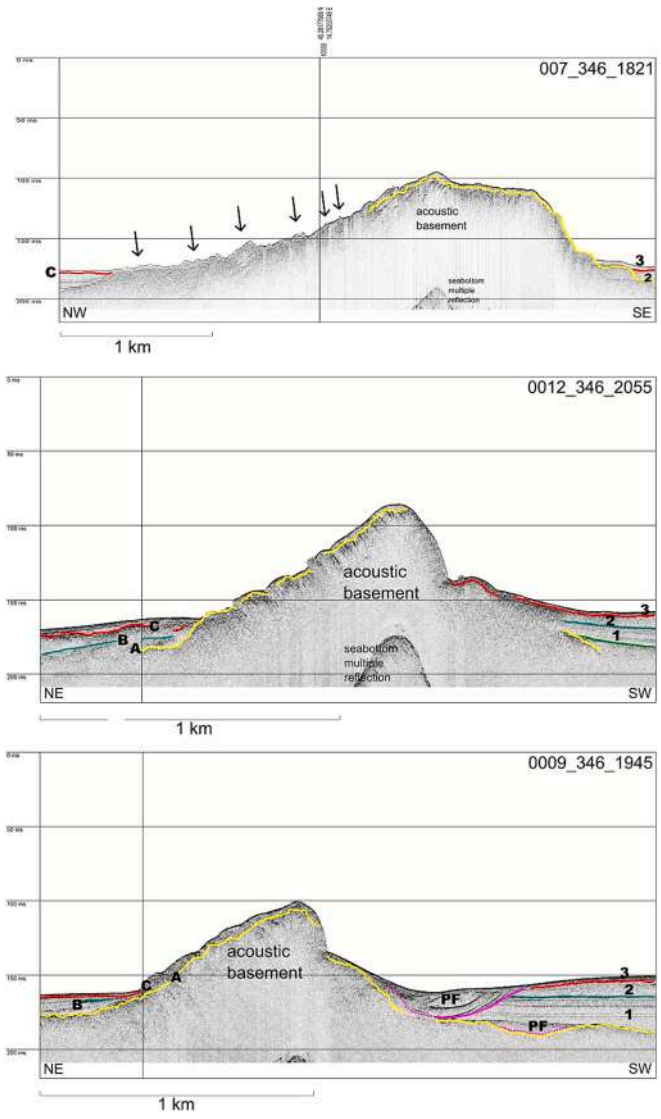

Fig. 4. Chirp profiles crossing the study area: profile 007_346_1821 is SE-NW oriented, while profiles 0012_346_2055 and 0009_346_1945 are SW-NE oriented. The acoustic basement, corresponding to the Miocene Cilento Flysch Group (Martelli et al., 2016), is indicated and the limit (yellow line) is marked by an angular unconformity. A. Quaternary units (1−2−3) and discontinuities among them (blue line B, red line C) are also indicated. PF indicates paleochannels filled by Quaternary sediment. (For interpretation of the references to colour in this figure legend, the reader is referred to the web version of this article.)

obtained during the pre-processing was used as input for classification, with the following thresholds: vertical cutoff = 0.23, minimum vertical threshold = 0.2, minimum width = 4, minimum width-to-length (W/L) ratio = 0, and buffer-to-delineation = 0.5. The output is a vector file containing the delineated seabed forms. A final manual revision step was required to verify the quality of the identified bedforms.

2.6. Morphometric parameters

Morphometric analysis was performed using CoMMa Toolbox v1.3 and the CoMMa Descriptor 2.0 tool (Arosio et al., 2024). A series of geometrical and statistical attributes was calculated for each feature. The "Basic Descriptors" tool calculates a set of geomorphometric parameters for each polygon feature, ranging from shape metrics to zonal statistics of slope, depth, and relative elevation compared to the global median. The "Texture Descriptors" tool provides additional metrics describing the surface quality, including zonal vector ruggedness measurement, aspect variability index, and, optionally, backscatter statistics. The "Volume Descriptors" tool estimates the relief and volume of each feature. These tools were used to characterize morphologies using the bathymetric surface (1 m resolution), shapefiles of seabed feature derived from semi-automated mapping, and backscatter data (60 cm resolution) for texture description.

3. Results

3.1. Seabed morphology of the study area

The study area ranged between 65 and 147 mwd (Fig. 2) and it corresponded to an elongated ridge with a gentle slope from the north to southwest and a steep slope towards northeast (Fig. 2a).

The seafloor surrounding the ridge was flat (Fig. 2a). Between 120 and 90 mwd the ridge was characterized by complex topography (Fig. 2a, black arrows), whereas between approximately 85 mwd and the top, the slope was more regular and gentler (Fig. 2a).

Between approximately 90 and 75 mwd (Fig. 2a, features area), the seafloor displayed, in its southwestern flank, mound-shaped morphologies that are sub-circular to polygonal in plan view (Fig. 2a, 3). In some instances, they appeared quite aligned in along directions consistent with the ones of the deepest rocky outcrops (Fig. 2a, black arrows, 3). The topographic profile in northwestern-southeaster direction (Fig. 3c) showed the occurrence of a series of bedforms which had asymmetry and a steep, higher side towards southeast than northwest. Interestingly, the topography of each feature seemed to range between conical (Fig. 3cA and C), rounded (Fig. 3cB) or squared (Fig. 3cD). The topographic profile in northeast-southwest direction (Fig. 3d) showed that the seafloor was gently steep with a wavy surface where the studied bedforms occurred (Fig. 4dC, F, G). Only E in Fig. 3d showed a squared profile.

Backscatter intensity was higher at shallower depth than at deeper depths (Fig. 2b). The studied bedforms exhibited a distinctive texture (Fig. 3b), with a high-reflectivity ring, not always completely closed, and a center that was characterized by low reflectivity (Fig. 3b).

3.2. Stratigraphy of the study area

CHIRP profile 007_346_1821 crossed the ridge in a northwest-to-southeast direction (see Fig. 1c for location), whereas profiles 0012_346_2055 (Figs. 1c, 4) and 0009_346_1945 (Figs. 1c, 4) crossed it in a southwest-to-northeast direction, orthogonal to the previous one. The stratigraphy of the sector outside the ridge showed a thicker sedimentary sequence (up to 20 m), composed of several seismo-stratigraphic units (Fig. 4). Based on seismo-stratigraphic criteria, three regional unconformities (A, B and C in Fig. 4) were identified, separating the seismo-stratigraphic units corresponding to the Quaternary deposits (1, 2, and 3 in Fig. 4). Profile 0009_346_1945 also revealed at least two paleochannels filled with sediments (PF in Fig. 4c). The ridge showed the acoustic basement, where the signal corresponds to a layered, inclined unit. The stratification exhibited an anti-dip slope towards the southwest and a dip-slope towards the northeast (Fig. 4b, c). The acoustic basement was locally exposed at the surface (Fig. 4a, black arrows), which corresponds to the sector characterized by high complex topography (Fig. 2a, black arrows), whereas it was overlain by a thin sedimentary layer (up to 5 m) at the ridge crest and along its flanks. Where visible, the contact between the top of the acoustic basement and the overlying sediments corresponded to an angular unconformity (Fig. 4, yellow lines).

3.3. ROV images of the study area

ROV 1 revealed a flat seascape, characterized by coarse-grained sediments containing abundant skeletal remains and sparse boxwork

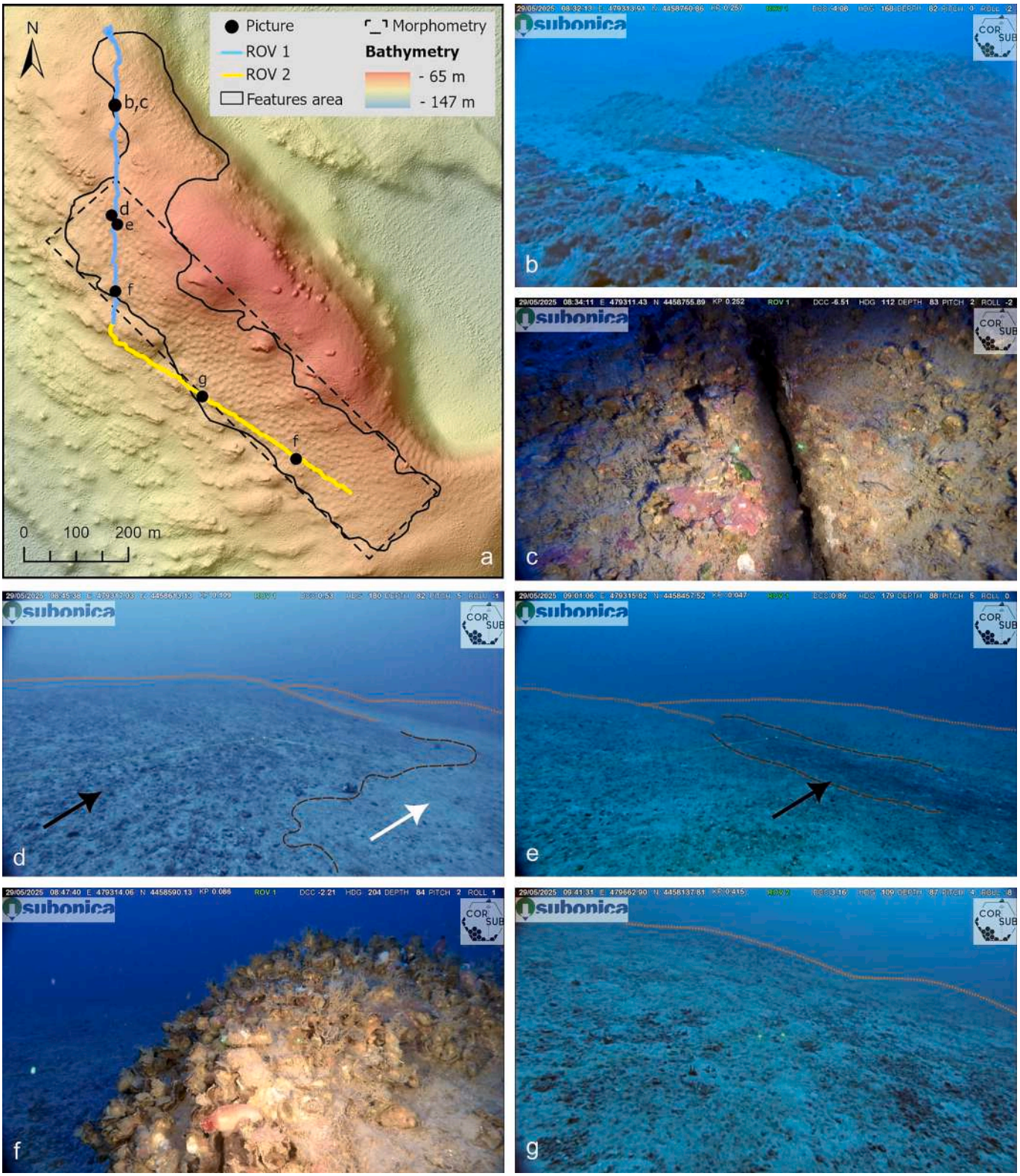

Fig. 5. Videoframes extracted from ROV 1 (b, c, d, e, f) and ROV 2 (g) with the indication of the localization on the studied ridge in a). a) view of the ridge and the studied bedforms with the ROV tracks (ROV 1 yellow and ROV 2 blue lines) and black points which indicate the position of the videoframes. Solid line outlines the zone with the studied bedforms. Dashed line outlines the zone used for morphometry in Figs. 6 and 7; b) rocky outcrops at one of the studied features; c) detail of the rocky outcrop with the encrusting benthic flora and fauna, in this case crustose coralline algae, bryozoans and sponges. d-e) wavy-profile seascape (orange dotted lines) showing the irregular distribution of coarse- and fine-grained sediments. Coarse fraction is marked by abundant boxwork rhodoliths on detrital coarse-grained biogenic sediment (brown dashed lines and black arrows in d) and e), whereas fine-grained sediments devoid of rhodoliths (white arrow in d); f) another example of a rocky outcrop showing heavy incrustations of benthic organism, in this case abundant bivalves; g) wavy-profile seascape (orange dotted line) in ROV 2 with sedimentary bottoms including abundant boxwork rhodoliths. b-h). In all frames, laser points as scale = 10 cm. (For interpretation of the references to colour in this figure legend, the reader is referred to the web version of this article.)

Table 1
Terrain attributes derived from the Digital Elevation Model, along with a description, the parameters used, and the tools employed for generation.

Terrain attribute	Parameters	Method	Relevance
Hillshade	Z factor = 1, 5	ArcGIS 10.5 – Spatial analyst	Increase the readability of elevation data by simulating a light source, showing shadows and illumination, and improve the visibility of features in low-relief areas.
Slope	Standard	ArcGIS 10.5 – Spatial analyst	Stability of sediments (grain size); local acceleration of currents (erosion, movement of sediments, creation of bedforms).
Aspect	Standard	ArcGIS 10.5 – Spatial analyst	Relation to direction of dominant geomorphic processes.
Curvature	Standard	ArcGIS 10.5 – Spatial analyst	Flow, channeling of sediments/currents, hydrological, and glacial processes; useful in the classification of landforms.
Fine Bathymetric Position Index (BPI)	Inner radius = 1, 3 Outer radius = 5, 15	Benthic Terrain Modeler (NOAA)	Fine scale BPI datasets are used to identify smaller benthic structures.
Terrain Ruggedness (VRM)	Neighborhood size = 3	Benthic Terrain Modeler (NOAA)	This method effectively captures variability in slope and aspect into a single measure. Ruggedness values in the output raster can range from 0 (no terrain variation) to 1 (complete terrain variation).
Relative deviation from mean value (RDMV)	Standard	TASSE Toolbox v. 1.1	This is a measure of relative position that identifies peaks (positive values) and pits (negative values).
Easterness (east)	Standard	TASSE Toolbox v. 1.1	This is a component of the aspect that informs on the orientation of the slope, i.e., its deviation from east. It ranges between −1 (fully West) and 1 (fully East).
Northerness (north)	Standard	TASSE Toolbox v. 1.1	This is the second component of the aspect that informs about the orientation of the slope, i.e., its deviation from north. It ranges between −1 (fully South) and 1 (fully North).
Standard Deviation (stdev)	Standard	TASSE Toolbox v. 1.1	This is a measure of rugosity/ruggedness/roughness.

rhodoliths (Fig. 5). At approximately 82 mwd, the ROV 1 encountered rocky outcrops (Fig. 5b), consisting of blocky sandstone partially encrusted by calcareous red algae and other benthic organisms (Fig. 5c). From points b and c in Fig. 5, the seafloor showed an increase in boxwork rhodoliths cover on a detrital coarse-grained biogenic sediment (Fig. 5d, e), and the seascape exhibited a wavy profile (Fig. 5d, e, orange dotted lines). The distribution of rhodoliths was uneven across the seafloor, allowing the distinction between bands of coarse-grained and fine-grained sediments (Fig. 5d, e, black and white arrows, brown-dashed lines). In addition, we observed sparse rocky outcrops, similar to the first outcrop, with heavy encrustation by calcareous benthic organisms, including abundant bivalves (Fig. 5f).

ROV 2 documented a seafloor sector marked by elongated rocky outcrops, whereas the surrounding sedimentary bottom was characterized by fine-grained sediments with sparse rhodoliths. At approximately 84 mwd, ROV 2 crossed a sector characterized by sediment rich in boxwork rhodoliths and other coarse-grained biogenic fragments (Fig. 5g). The seascape exhibited a wavy profile (Fig. 5g, orange-dotted line) corresponding to the studied mound-like features. Interestingly the wavy profile of Fig. 5g was observed when the ROV was exploring the seafloor in a northwest-to-southest direction, comparable to the direction of the topographic profile in Fig. 3d, which presented the same characteristics.

3.4. *Terrain parameters and geomorphometry of the targeted bedforms*

The results of the terrain variable and attribute analyses provided improved visualization of the studied bedforms and enabled a quantitative description of their characteristics (Fig. 6). Analysis of the bathymetric data (Figs. 3, 6a) revealed a mound-shaped morphology. Based on SSS imagery (Figs. 3, 6b) and reflectivity data (Fig. 6c), they exhibited a distinctive texture: a high-reflectivity ring, not always fully closed, with a center of lower reflectivity (Fig. 3b). This pattern was spatially consistent, producing a sub-polygonal texture, that resembles a beehive (Figs. 3b, 6b red arrows, 6c red arrows). The slope map (Fig. 6d) showed that the studied bedforms are asymmetric, with a flat upslope portion towards north-to-northwest truncated by a steep, curved, downslope towards northeast (Fig. 6d black arrow) to southeast (Fig. 6d red arrow). The aspect map (Fig. 6e) indicated a west-to-northwest orientation. These morhologies contributed to a local increase in terrain ruggedness (Fig. 6f) and standard deviation (Fig. 6g). The deviation from mean elevation was also clearly expressed, with higher values corresponding to the peaks of the studied bedforms (Fig. 6h, red arrows).

The mean-derived LTP results quantify how elevated or low-lying a site is relative to local topographic variability (Fig. 7a), and the studied bedforms corresponded to seafloor segments associated with high LTP values.

Semi-automatic mapping identified 565 seabed bedforms within an area of ca. 15 ha (Fig. 7b). For these polygonal features, morphometric analysis yielded 20 parameters, a subset of which is reported in Table 2 and Fig. 8. They had a mean length of 8.62 ± 2.9 m (range: 2.03–24.16 m), a mean width of 6.14 ± 1.82 m (range: 2.20–10.80 m) and a mean height of 0.41 ± 0.16 m (range: 0.14–1.11 m). The elongation ratio was 1.44 ± 0.41 (range: 1.00–4.81). The perimeter had a mean value of 23.92 ± 7.16 m (range: 6.67–58.45 m) and a mean area of 44.28 ± 23.90 m^2 (range: 3.48–167.80 m^2). Volume ranged between 3.9 and 46.14 m^3 (range: 12.06 ± 7.27 m^3). The orientation ranged between 0° and 180° (north-to-south); however, 306 out of 565 polygons were oriented between northeast and southeast. Calculated slope ranged between 0.1° and 33° degrees, with a mean value of 5.7 ± 2.1°. Circularity ranged between 0.47 and 0.99, whereas rectangularity ranged between 0.60 and 0.89.

4. Discussion

Reef development is inherently patchy across spatial and temporal

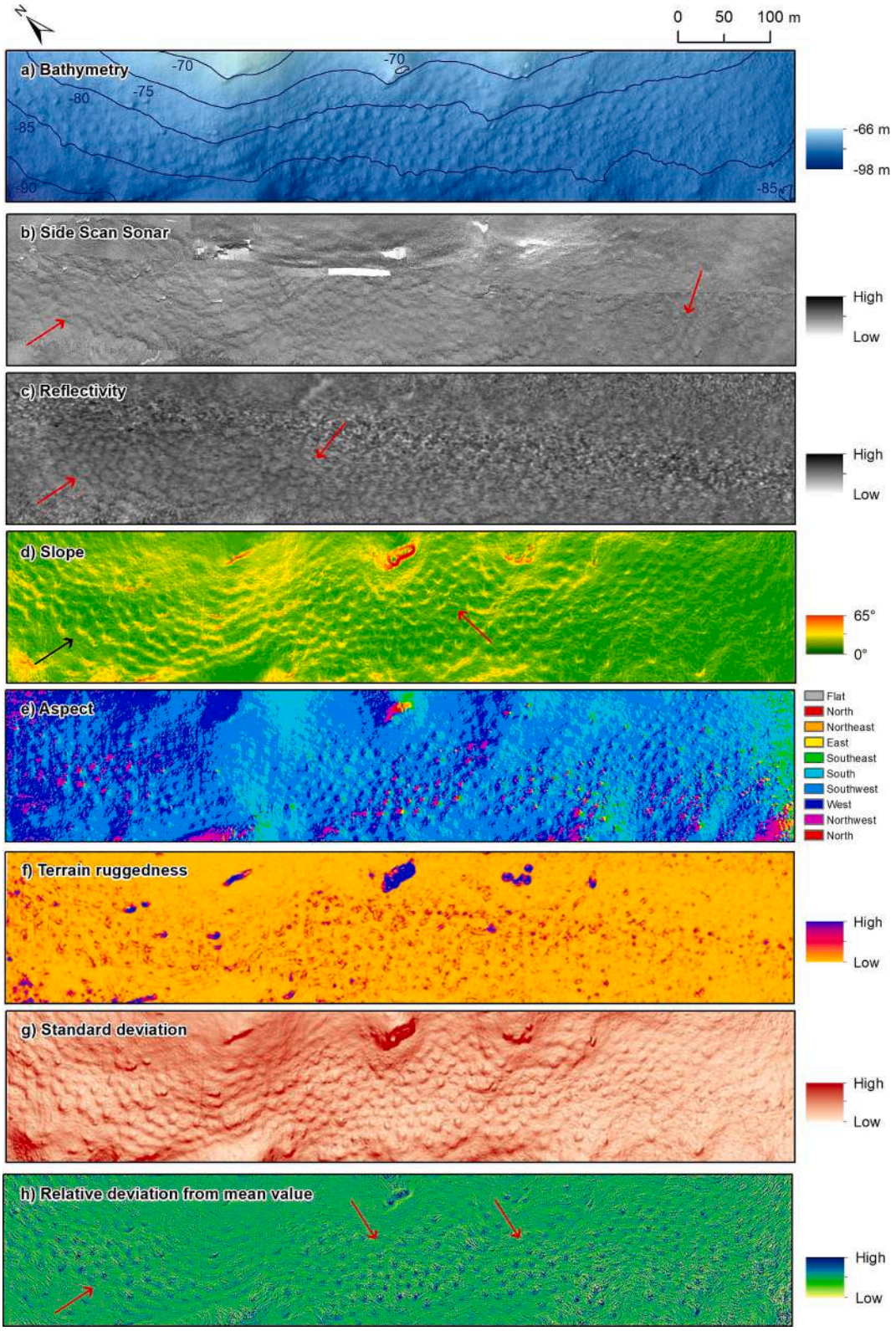

Fig. 6. Maps of the terrain variables and attributes extracted for the studied zone (see Fig. 5 for location). a) Bathymetric surface (1 m resolution) on shared relief (Z factor = 5 and isobaths = 5 m contour); b) Acoustic image from Side Scan Sonar (SSS) (20 cm resolution). Red arrows indicate the peculiar texture described in the text. c) Seafloor reflectivity from multibeam backscatter (60 cm resolution). Red arrows indicate the peculiar texture described in the text. d) Slope in degree. Red arrows indicate the northwest to southwest position of the steepest portion of each feature. e) Aspect measured as a compass direction (azimuth) in degrees from true north; f) Terrain ruggedness identifying rugosity in the benthic terrain environment; g) Standard deviation measuring the rugosity/ruggedness/roughness; h) Relative deviation from mean value measuring the relative position, that means identify peaks (higher values) and pits (lower values). Red arrows indicate where the relative standard deviation is high due to the occurrence of a complex topography on the sea floor, corresponding to the studied bedforms. (For interpretation of the references to colour in this figure legend, the reader is referred to the web version of this article.)

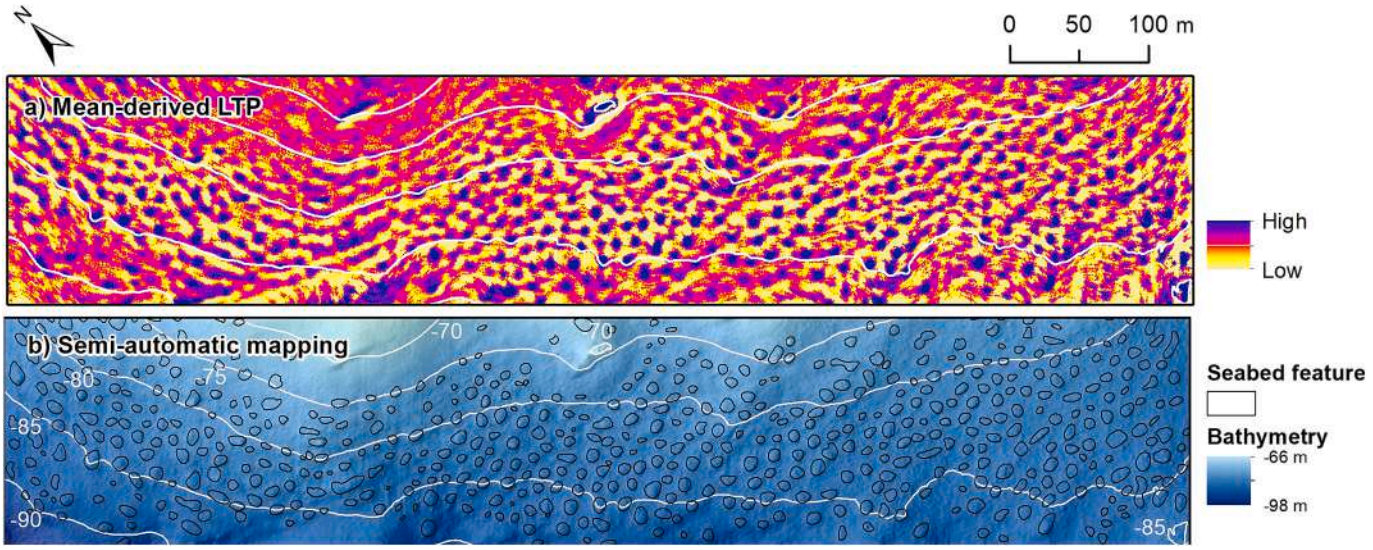

Fig. 7. a) Mean-derived Local Topographic Position quantifying how elevated or low-lying a site is relative to the local topographic variability. b) Map of the seabed morphologies, identified with the semi-automatic process, displayed on the bathymetric surface and with isobaths (white lines).

Table 2
Morphometric parameters of the studied bedforms extracted using the CoMMa toolbox and descriptor. N° counting indicates the numbers of structures considered for each parameter. Values are expressed as mean value (mean), standard deviation (sd), minimum (min) and maximum (max) values.

	n° counting	mean	sd	min	max
Length	565	8.62	2.90	2.03	24.16
Width	564	6.14	1.82	2.02	10.80
Elongation ratio	565	1.44	0.41	1.00	4.82
Orientation	494	76.83	55.87	0.00	170.50
Perimeter	565	23.93	7.16	6.67	58.46
Area	565	44.28	23.90	3.48	167.08
Circularity	565	0.91	0.08	0.47	0.99
Rectangularity	565	0.79	0.03	0.60	0.89
Volume	90	12.07	7.27	3.91	46.14
Relief	90	0.42	0.16	0.15	1.12
Slope_MIN	565	2.0	1.8	0.1	11.0
Slope_MAX	565	10.8	4.0	0.9	33.2
Slope_MEAN	565	5.7	2.1	0.9	16.3

scales (Mumby and Edwards, 2002); often exhibiting fractal patterns that influence benthic community distribution (Purkis et al., 2006). In spatial analyses, a "patch" is defined as a discrete, relatively homogeneous domain with properties distinct from those of surrounding areas (Rankey, 2002). Patch shapes, quantified using morphometric parameters such as elongation and circumscribed circle metrics, can reveal differences in structural complexity. Reef development is a gradual process influenced by oceanographic, sedimentary, and tectonic factors over long timescales. Consequently, the geological history of the substrate is critical for understanding benthic patterns.

Mesophotic bioconstructions with patchy seafloor distributions are widespread in the Mediterranean (Bonacorsi et al., 2012; Aksu et al., 2018). Along the coast of the Campania Region, rhodalgal reefs and rhodolith beds are abundant (Toscano et al., 2006; Bracchi and Basso, 2012; Aiello, 2020a, 2020b); however, none exhibit the peculiar pattern observed at Cape Licosa. Given evidence from 2004 of a repeated geometric texture in space, and the collected material potentially corresponds to bioconstructions of crustose coralline algae, we hypothesized that the origin of the Cape Licosa morphologies may be related to these concepts.

CORSUB data confirm the persistence of these bedforms over more than 20 years. They are evident on the bathymetry and backscatter data (Figs. 2, 3, 5, 7). ROV images show that the seafloor has a wavy profile with variable substrate composition: rocks encrusted by coralline algae, bryozoans, and bivalves, as well as coarse-grained sediments rich in boxwork rhodoliths (Fig. 5). Sediment distribution is controlled by interactions between topography and bottom currents; however, it does not extend uniformly across the investigated site (Fig. 5) and cannot univocally account for the peculiar morphology or texture observed (Figs. 3, 7). Notably, a weak correspondence exists between individual bedform and the type of sediment. Most of them correspond to mound-shaped accumulation of coarse-grained sediments, including boxwork rhodoliths (Fig. 5), whereas only in rare cases do they correspond to rocks encrusted with calcareous red algae, bryozoans, and bivalves (Fig. 5). These mound-shaped morphologies occur on the gently inclined summit of a ridge, between approximately 75 and 90 mwd, exhibiting an asymmetric, low-relief aspect with mean dimensions of 8.6 × 6.1 × 0.4 m (Figs. 3, 4, 5, 9; Table 2). The upslope flank of each feature is generally gentle, whereas the downslope edge is steeper (Figs. 3, 6), and they show a conical, rounded or squared outlines in northwest-to-southeast direction (Fig. 3c)

4.1. Origin of the studied seabed morphologies

Because no direct correlation exists between the studied structures and specific sediment type or habitat at seafloor, the origin of this occurrence must be reconstructed by considering additional factors, from a long-term perspective (Fig. 9).

In the Cape Licosa area, Quaternary sea-level fluctuations led to alternating phases of subaerial exposure and marine transgression, influencing sedimentary regimes and providing opportunities for biogenic activity (Savini et al., 2021). In particular, the Last Glacial Maximum reached a paleodepth exceeding 140 mwd in an area considered tectonically stable (Lambeck et al., 2004). Consequently, the study area including the ridge experienced prolonged subaerial exposure (Fig. 9b). Sub-bottom profiles clearly show an acoustically-transparent basement (Figs. 4; 9a) corresponding to the Miocene Cilento Flysch Group (Martelli et al., 2016), overlain by a thin Holocene sediment drape (Figs. 4; 9a). The contact between the two is an angular unconformity corresponding to an irregular paleosurface over which sediment has accumulated during the last millennia (Figs. 4; 9a). Filled paleochannels in the stratigraphy (Fig. 3 PF) further indicate intense erosion during low-stand phases, consistent with regional records (Amorosi et al., 2012; Aiello et al., 2017; Iorio et al., 2024). Subaerial erosion of stratified rocks, such as the Cilento flysch group, at LGM could

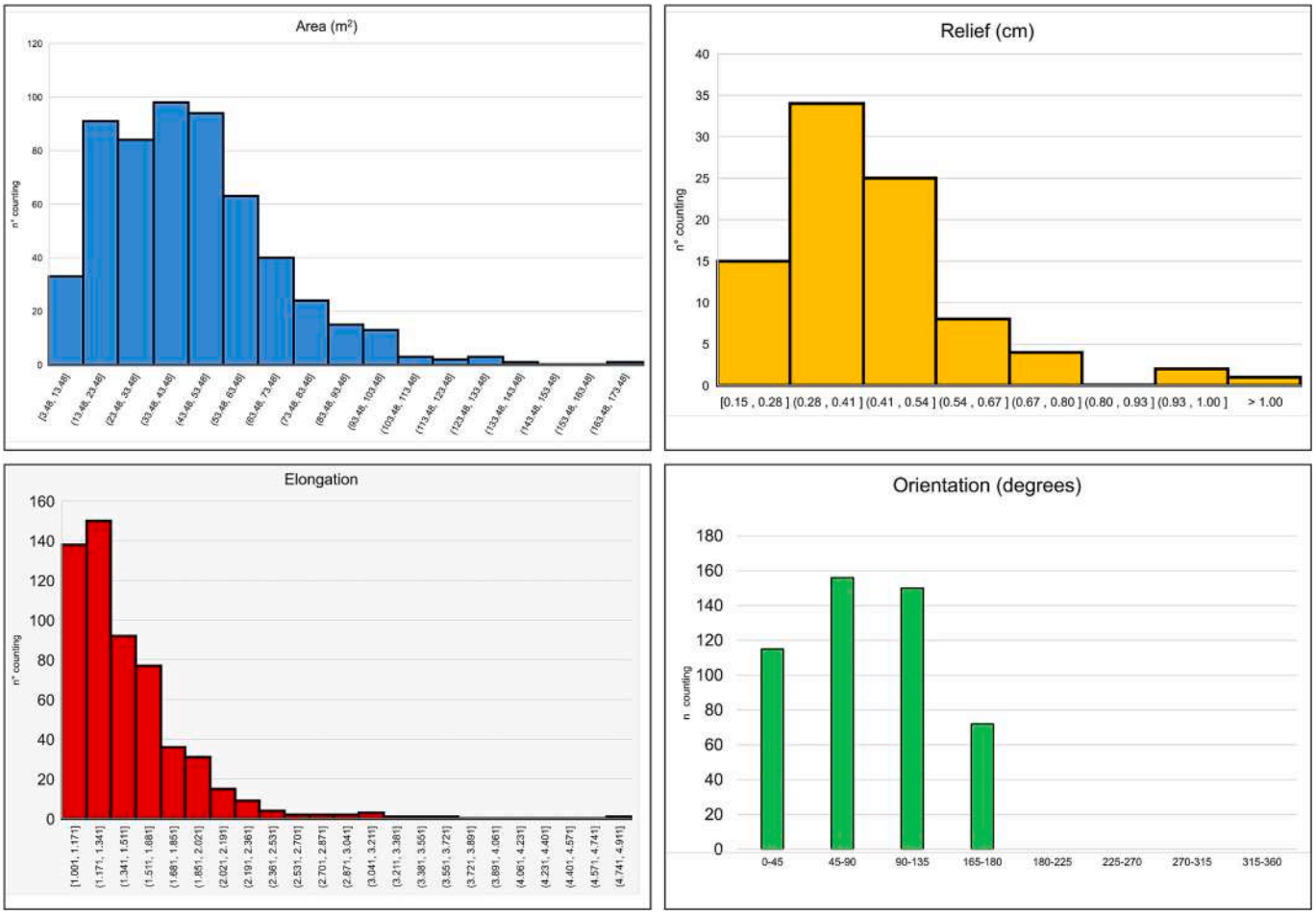

Fig. 8. Histograms of the distribution of some of the parameters extracted using the CoMMa toolbox and descriptor: Area in square meters, Relief in cm, Elongation in m and bar-graph for the Orientation in degrees with respect to the N.

have generate the basal complex topography (Fig. 9b), which is similar to the outcrops we can observe today along the coastline of Cape Licosa (Valente et al., 2017).

4.2. Development of the studied seabed morphologies

During the Holocene sea-level rise, the sediment distribution and accumulation patterns were likely controlled by interactions among the paleo-topography generated during LGM, sediment transport, in situ sediment production, and bottom currents. However, the resolution of seismic data does resolve distinct recognizable events within the sediment package deposited during the Holocene at the study area (Fig. 4). Preliminary results from box-corers indicate an alternation of muddy sand and biogenic gravelly sand, with the occurrence of fossil rhodolith beds (Bazzicalupo et al., 2025). Present-day sedimentation is characterized by coarse-grained biogenic material; boxwork rhodoliths; and sparse coralligenous-bivalve reefs where rocks outcrop (Fig. 5). Therefore, it is likely that Holocene sedimentation covered this complex paleo-topographic surface, inheriting its shape (Fig. 9c-e). Where the bedrock is exposed and significant bioengineer activity is present, it corresponds to one of these mounded structures (Fig. 9e). By contrast, the others correspond to asymmetrical bedforms described in this study (Figs. 5; 9d), which have inherited their shape from the underlying paleosurface (Fig. 9d). Irregular alternations of coarse-grained sediments rich in boxwork rhodoliths and areas largely devoid of such material (Fig. 5) correlate with the sub-geometric, patchily, textures observed in SSS and backscatter data (Figs. 3; 6). This pattern may indicate a link between these seabed morphologies and sedimentation with hydrodynamics, reported as potentially intense in this area (De Ruggiero et al., 2016, 2020). Notably, in the deepest parts of the ridge (between 90 and 120 mwd, Fig. 2), where the sedimentary cover is thinner or null, rocky substrate still outcrops forming mound-like profiles (Fig. 9a, white arrows) similar to those examined in this study but lacking Holocene sedimentary cover.

Finally, the ridge in the study area is an elevated structure, which represents an ideal setting in mesophotic environments for the formation of ì rhodolith beds (Basso et al., 2017). In this case, the accumulation of sediments over a complex paleosurface can give rise to bottom forms of varying stability that interact with a driving force such as a current. This interaction likely helps maintain the wavy seafloor profile observed in the area and support rhodolith development.

4.3. A synthesis of present knowledge

Based on these considerations, we propose that the enigmatic bedforms at Cape Licosa result from Holocene sediment draping over a rugged, LGM-eroded rocky substrate (Fig. 9). Subsequent sediment redistribution by bottom currents, coupled with opportunistic colonization by bioengineers such as coralline algae and bivalves, resulted in the formation of the observed beehive patterns. Coarse-grained biogenic sediments, including rhodoliths, have also contributed to the present configuration of the mesophotic seabed (Figs. 2, 3 and 5). This interpretation emphasizes the combined influence of paleo-topography, post-glacial sedimentary processes and benthic colonization in shaping seabed morphology in Mediterranean mesophotic environments.

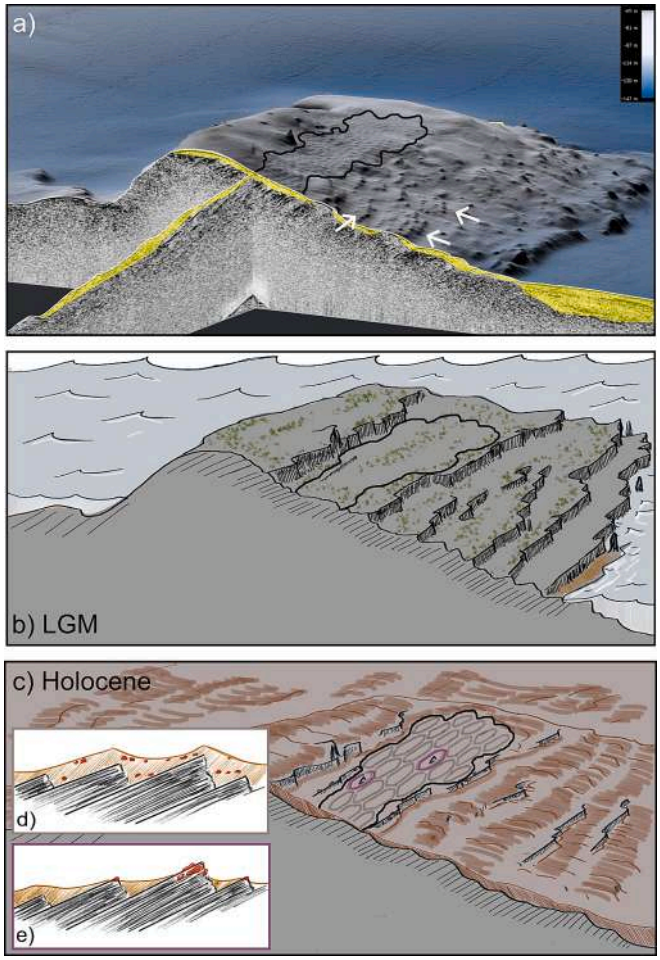

Fig. 9. A model of the origin and development of the studied bedforms. a) 3D visualization of the bathymetry of the ridge from northwest, cut in correspondence of the chirp profile 0012_346_2055 and 007_346_1821, both also in Fig. 4. The irregular, Holocene sedimentary drape is marked in yellow. Black line outlines the features area. White arrows indicate deeper rocky outcrops which present morphology similar to the studied morphologies, but they do not show any cover by Holocene sediments; b) a model of the ridge during the Last Glacial Maximum, during which subaerial erosional processes contributed to the formation of a complex topography. Black line outlines the features area. c) a model of the ridge as it looks like today. Black line outlines the features area, which includes both wavy-shaped bedforms with (gray) and without (purple) rocky outcrops. d) a sketch of the studied bedforms where they correspond to wavy-shaped sediments on the rocky substrates. e) a sketch of the studied bedforms where they include the outcrop of the rocky substrates coved by encrusting organisms. (For interpretation of the references to colour in this figure legend, the reader is referred to the web version of this article.)

5. Conclusions

The enigmatic seabed morphologies offshore Cape Licosa are the product of complex interactions among inherited paleo-topography, Quaternary sedimentary processes, and benthic colonization. Formed on a rugged LGM-eroded Cilento Flysch substrate, and subsequently draped by a thin Holocene sedimentary layer, these mounded, subcircular to polygonal morphologies have been shaped by bottom currents and opportunistic bioengineers, including coralline algae and bivalves. Their geometric arrangement and persistence highlight the combined influence of geological history, hydrodynamic forcing, and biogenic activity in shaping mesophotic seabed morphology along the Mediterranean continental shelf.

Funding informations

This work was funded by the European Union - Next Generation EU, Mission 4, Investment 1.1 of the national recovery and resilience plan trough the Italian call “PRIN 2022”. This project is coded PRIN n°2022RKHBMB (CUP H53D23001620006).

CRediT authorship contribution statement

Valentina Alice Bracchi: Visualization, Validation, Supervision, Resources, Project administration, Methodology, Investigation, Funding acquisition, Formal analysis, Data curation, Conceptualization, Writing – review & editing, Writing – original draft. **Sara Innangi:** Software, Methodology, Investigation, Formal analysis, Data curation, Writing – original draft. **Renato Tonielli:** Investigation, Writing – review & editing. **Gemma Aiello:** Formal analysis, Data curation, Writing – review & editing. **Daniela Basso:** Investigation, Writing – review & editing. **Davide Vernazzani:** Data curation, Writing – review & editing. **Valentina Grande:** Validation, Software, Project administration, Methodology, Funding acquisition, Formal analysis, Data curation, Writing – original draft. **Pietro Bazzicalupo:** Writing – review & editing.

Declaration of competing interest

The authors declare that they have no known competing financial interests or personal relationships that could have appeared to influence the work reported in this paper.

Acknowledgements

The authors would like to thank the editor Michele Rebesco and three anonymous reviewers for their valuable revisions of the first version of the manuscript. We would also like to express our sincere gratitude to the colleagues of the TREMOR cruise for their professional collaboration in the collection of data during the campaign, and the the captains and crews of the R/V Gaia Blu. We also thank Riccardo Arosio, PhD, for his help in the use of the CoMMa Toolbox.

Data availability

Data are findable and accessible in the Seamap metadata catalog at: http://seamap-catalog.data.ismar.cnr.it:8080/geonetwork/corsub. Biodiversity data are also integrated into the Geoportal for Marine Biodiversity in Italy, available through the Italian Biodiversity Gateway (https://www.biodiversitygateway.it/en/biodiversity-solutions/marine-biodiversity-geoportal-species-habitats-and-coastal-areas).

References

Aiello, G., 2019. Elaborazione ed interpretazione geologica di sismica di altissima risoluzione nell'offshore del Promontorio del Cilento (Tirreno meridionale, Italia). Quaderni di Geofisica 155, 1–24.

Aiello, G., 2020a. New sedimentological and coastal and marine geological data on the Quaternary marine deposits of the Ischia Island (Gulf of Naples, Southern Tyrrhenian Sea, Italy). Geomar. Lett. 40, 593–618.

Aiello, G., 2020b. Bioclastic deposits in the NW Gulf of Naples (Southern Tyrrhenian Sea, Italy): a focus on new sedimentological and stratigraphic data around the Island of Ischia. In: Geochemistry. IntechOpen. https://doi.org/10.5772/intechopen.95083. Available from:

Aiello, G., Caccavale, M., 2021. The Depositional Environments in the Cilento Offshore (Southern Tyrrhenian Sea, Italy) based on Marine Geological Data. J. Mar. Sci. Eng. 9, 1083. https://doi.org/10.3390/jmse9101083.

Aiello, G., Caccavale, M., 2023. A Seismo-Stratigraphic Analysis of the Relict Deposits of the Cilento Continental Shelf (Southern Italy). Proceedings 87, 10. https://doi.org/10.3390/IECG2022-14296.

Aiello, G., Caccavale, M., 2024. Seismo-Stratigraphic Data of Wave-Cut Marine Terraces in the Licosa Promontory (Southern Tyrrhenian Sea, Italy). Coasts 4, 392–418. https://doi.org/10.3390/coasts4020020.

Aiello, G., Caccavale, M., 2025. The relict deposits of the Cilento offshore (Southern Tyrrhenian Sea, Italy) based on seismo-stratigraphic data. Bull. Region. Nat. Hist. 5 (1), 1–18. https://doi.org/10.6093/2724-4393/12459.

Aiello, G., Insinga, D.D., Iorio, M., Meo, A., Senatore, M.R., 2017. On the occurrence of the Neapolitan Yellow Tuff tephra in the Northern Phlegraean Fields offshore (Eastern Tyrrhenian margin; Italy). Ital. J. Geosci. 136 (2), 263–274. https://doi.org/10.3301/IJG.2017.06.

Aksu, A.E., Hiscott, R.N., Kostylev, V.E., Yaltırak, C., 2018. Organized patches of bioherm growth where the Strait of Dardanelles enters the Marmara Sea, Turkey. Palaeogeogr. Palaeoclimatol. Palaeoecol. 490, 325–346. https://doi.org/10.1016/j.palaeo.2017.11.010.

Amorosi, A., Pacifico, A., Rossi, V., Ruberti, D., 2012. Late Quaternary incision and deposition in an active volcanic setting: the Volturno valley fill, southern Italy. Sediment. Geol. 282, 307–320.

Antonioli, F., Cinque, A., Ferranti, L., Romano, P., 2004. Emerged and submerged Quaternary marine terraces of Palinuro Cape (Southern Italy). Mem. Descr. Carta Geol. Ital. LII, 237–260.

Arosio, R., Gafeira, J., De Clippele, L.H., Wheeler, A.J., Huvenne, V.A.I., Sacchetti, F., Conti, L.A., Lim, A., 2024. CoMMa: a GIS geomorphometry toolbox to map and measure confined landforms. Geomorphology 458, 109227. https://doi.org/10.1016/j.geomorph.2024.109227.

Ballesteros, E., 2006. Mediterranean coralligenous assemblages. In: Barners, H. (Ed.), Mar. Biol. Ann. Rev. LTD Press, London, EN, pp. 123–195. https://doi.org/10.1201/9781420006391.ch4.

Basso, D., Babbini, L., Ramos Esplá, A., Salomidi, M., 2017. Mediterranean rhodolith beds. In: Riosmena-Rodríguez, R., Nelson, W. Wendy, Aguirre, J. (Eds.), Rhodolith/maërl beds: a global perspective, pp. 281–298.

Bazzicalupo, P., Tonielli, R., Grande, V., Innangi, S., Basso, D., Felsani, M., et al., 2025. Anomalous seafloor morphologies: insights from the CORSUB Project (Tyrrhenian Sea, Italy). In: Abstract EGU25. https://doi.org/10.5194/egusphere-egu25-18832.

Bonacorsi, M., Pergent-Martini, C., Clabaut, P., Pergent, G., 2012. Coralligenous "atolls": Discovery of a new morphotype in the Western Mediterranean Sea. C. R. Biol. 335 (10–11), 668–672. https://doi.org/10.1016/j.crvi.2012.10.005.

Böttner, C., Hoffmann, J.J.L., Unverricht, D., Schmidt, M., Spiegel, T., Geersen, J., et al., 2024. The enigmatic pockmarks of the sandy southeastern North Sea. Geochem. Geophys. Geosyst. 25, e2024GC011837. https://doi.org/10.1029/2024GC011837.

Bracchi, 2006. Tanatocenosi a molluschi associate a morfologie sommerse di origine problematica (Punta Licosa, Campania). Unpublished thesis. University of Milano-Bicocca, Milan, Italy.

Bracchi, V.A., Basso, D., 2012. The contribution of calcareous algae to the biogenic carbonates of the continental shelf: Pontian Islands, Tyrrhenian Sea, Italy. Geodiversitas 34 (1), 61–76. https://doi.org/10.5252/g2012n1a4.

Bracchi, V.A., Basso, D., Marchese, F., Corselli, C., 2017. Coralligenous morphotypes on subhorizontal substrate: a new categorization. Cont. Shelf Res. 144, 10–20.

D'Angelo, S., Di Stefano, F., Fiorentino, A., Lettieri, M.T., Russo, G.F., Violante, C., 2020. Marine landscapes and habitats of Cilento Geopark (Italy) - linking geo- and biodiversity using a multiscalar approach. In: Harris, P.T., Baker, E. (Eds.), Seafloor Geomorphology as Benthic Habitat, 2nd ed. Elsevier, Amsterdam, The Netherlands, pp. 421–437.

De Pippo, T., Pennetta, M., 2000. Late Quaternary morphological evolution of a continental margin based on emerged and submerged morphostructural features: the south-eastern Tyrrhenian margin (Italy). Zeit. Geomorph. N. F. 44, 435–448.

De Ruggiero, P., Esposito, G., Napolitano, E., Iacono, R., Pierini, S., Zambianchi, E., 2016. Modelling the marine circulation of the Campania coastal system (Tyrrhenian Sea) for the year 2016: analysis of the dynamics. J. Mar. Syst. 210, 103388.

De Ruggiero, P., Napolitano, E., Iacono, R., Pierini, S., 2020. A high-resolution modelling study of the circulation along the Campania coastal system, with a special focus on the Gulf of Naples. Cont. Shelf Res. 122, 85–101. https://doi.org/10.1016/j.csr.2016.03.026 02.

Deiana, G., Lecca, L., Melis, R.T., Soldati, M., Demurtas, V., Orrù, P.E., 2021. Submarine Geomorphology of the Southwestern Sardinian Continental Shelf (Mediterranean Sea): Insights into the last Glacial Maximum Sea-Level changes and Related Environments. Water 13 (2), 155. https://doi.org/10.3390/w13020155.

Di Geronimo, I., Di Geronimo, R., Rosso, A., Sanfilippo, R., 2002. Structural and taphonomic analyses of a columnar coralline algal build-up from SE Sicily. Geobios 24, 86–95. https://doi.org/10.1016/S0016-6995(02)00050-5.

EMODnet Seabed Habitats product, 2023. Contains data from the Global Distribution of Seagrasses (v7.1 March 2021). UNEP-WCMC, Short FT (2021). Global Distribution of Seagrasses (Version 7.1). Seventh Update to the Data Layer Used in Green and Short (2003). UN Environment World Conservation monitoring Centre. Data, Cambridge (UK). https://doi.org/10.34892/x6r3-d211.

Ferraro, L., Pescatore, T.S., Russo, B., Senatore, M.R., Vecchione, C., Coppa, M.G., Di Tuoro, A., 1997. Studi di geologia marina sul margine tirrenico: La piattaforma continentale tra Licosa Cape e Capo Palinuro (Tirreno meridionale). Boll. Soc. Geol. Ital. 116, 473–485.

Foglini, F., Angeletti, L., Campiani, E., Grande, V., Leidi, E., Madricardo, F., et al., 2015. Habitat mapping in the Adriatic (Mediterranean Sea): Approaches and methodologies for assessing seafloor habitat from coastal areas to deep sea. In: *Convegno "La Geologia Marina in Italia", Primo Convegno dei Geologi Marini Italiani*, 18–19 febbraio 2016, Roma, Italy.

Grande, V., Proietti, R., Foglini, F., Remia, A., Correggiari, A., Paganelli, D., et al., 2015. Sistema Informativo per il monitoraggio ambientale della risorsa sabbia offshore nei progetti di protezione costiera: geodatabase env_Sand. ISPRA, Manuali e Linee Guida, 127/2015, 63 pp.

Harris, P.T., 2020. Seafloor geomorphology—Coast, shelf, and abyss. In: Harris, Peter T., Baker, Elaine (Eds.), Seafloor Geomorphology as Benthic Habitat, Second edition. Elsevier, pp. 115–160.

Innangi, S., Bracchi, V.A., Basso, D., Tonielli, R., 2025. Caught in the act: calcareous algae creating undescribed morphologies of mesophotic algal reef. Mar. Geol. 490, 107644. https://doi.org/10.1016/j.margeo.2025.107644.

Iorio, M., Meo, A., Aiello, G., Senatore, M.R., 2024. The Neapolitan Yellow Tuff record in the Gaeta Gulf (Eastern Tyrrhenian margin, Southern Italy). Adv. Geosci. 63, 15–27. https://doi.org/10.5194/adgeo-63-15-2024.

Lambeck, K., Antonioli, F., Purcell, A., Silenzi, S., 2004. Sea-level change along the Italian coast for the past 10,000 yr. Quat. Sci. Rev. 23, 1567–1598.

Lambeck, K., Antonioli, F., Anzidei, M., Ferranti, L., Leoni, G., Scicchitano, G., Silenzi, S., 2011. Sea level change along the Italian coast during the Holocene and projections for the future. Quat. Int. 232, 250–257.

Lecours, V., 2017. TASSE (Terrain Attribute selection for Spatial Ecology) Toolbox v. Version 1.1. https://doi.org/10.13140/RG.2.2.15014.52800.

Lecours, V., Dolan, M.F.J., Micallef, A., Lucieer, V.L., 2016. A review of marine geomorphometry, the quantitative study of the seafloor. Hydrol. Earth Syst. Sci. 20, 3207–3244. https://doi.org/10.5194/hess-20-3207-2016.

Lindsay, J.B., Cockburn, J.M.H., Russell, H.A.J., 2015. An integral image approach to performing multi-scale topographic position analysis. Geomorphology 245, 51–61. https://doi.org/10.1016/j.geomorph.2015.05.025.

Martelli, L., Nardi, G., Cammarosano, A., Cavuoto, G., Aiello, G., D'Argenio, B., Marsella, E., 2016. Note Illustrative Della Carta Geologica d'Italia Alla Scala 1: 50,000; Regione Campania. ISPRA (Servizio Geologico d'Italia), Rome, Italy, pp. 1–110 (accesso 28 marzo 2025). Disponibile online: http://www.isprambiente.gov.it/Media/carg/noteillustrative/502_Agropoli.pdf.

Meredyk, S.P., Edinger, E., Piper, D.J.W., Huvenne, V.A.I., Hoy, S., Ruffman, A., 2020. Enigmatic deep-water mounds on the Orphan Knoll, Labrador Sea. Front. Mar. Sci. 6, 744. https://doi.org/10.3389/fmars.2019.00744.

Micallef, A., Foglini, F., Le Bas, T., Angeletti, L., Maselli, V., Pasuto, A., Taviani, M., 2013. The submerged palaeolandscape of the Maltese Islands: Morphology, evolution and relation to Quaternary environmental change. Mar. Geol. 335, 129–147.

Mumby, P.J., Edwards, A.J., 2002. Mapping marine environments with IKONOS imagery: enhanced spatial resolution can deliver greater thematic accuracy. Remote Sens. Environ. 82 (2–3), 248–257. https://doi.org/10.1016/S0034-4257(02)00041-X.

Parsons, D.R., Monterey Coordinated Canyon Experiment Team & Bute Inlet Monitoring Team, 2019. Enigmatic Bedforms in the Deep Sea. In: *Marine and River Dune Dynamics – MARID VI*, 1–3 Aprile 2019, Bremen, Germany.

Pennetta, M., Bifulco, A., Savini, A., 2013. Ricerca di depositi di sabbia sottomarina relitta sulla piattaforma continentale del Cilento (SA) utilizzabile per interventi di ripascimento artificiale dei litorali. Geol. Ambiente Suppl. S1, 1–21.

Pike, R.J., Dikau, R., 1995. Advances in geomorphometry-proceedings of the Walter F. Wood Memorial Symposium. Z. Geomorphol. Suppl. 101, 1–328. ISBN 978–3–443-21101-1.

Pike, R.J., Evans, I.S., Hengl, T., 2009. Geomorphometry: A Brief Guide. In: Hengl, T., Reuter, H.I. (Eds.), Developments in Soil Science. Elsevier Science Publishers, Amsterdam, pp. 3–30. https://doi.org/10.1016/S0166-2481(08)00001-9.

Purkis, S.J., Riegl, B., Dodge, R.E., 2006. Fractal patterns of coral communities: evidence from remote sensing (Arabian Gulf, Dubai, U.A.E.). In: *Marine & Environmental Sciences Faculty Proceedings, Presentations, Speeches, Lectures*, 13.

Rankey, E.C., 2002. Spatial patterns of sediment accumulation on a Holocene carbonate tidal flat, Northwestern Andros Island, Bahamas. J. Sediment. Res. 72 (5), 591–601.

Savini, A., Basso, D., Bracchi, V.A., Corselli, C., Pennetta, M., 2012. Maerl-bed mapping and carbonate quantification on submerged terraces offshore the Cilento peninsula (Tyrrhenian Sea, Italy). Geodiversitas 34, 77–98.

Savini, A., Bracchi, V.A., Cammarosano, A., Pennetta, M., Russo, F., 2021. Terraced Landforms Onshore and Offshore the Cilento Promontory (South-Eastern Tyrrhenian margin) and their significance as Quaternary Records of Sea Level Changes. Water 13, 566. https://doi.org/10.3390/w13040566.

Toscano, F., Vigliotti, M., Simone, L., 2006. Variety of coralline algal deposits (rhodalgal facies) from the Bays of Naples and Pozzuoli (northern Tyrrhenian Sea, Italy). In: Pedley, H.M., Carannante, G. (Eds.), Cool-Water Carbonates: Depositional Systems and Palaeoenvironmental Controls, 255. Geological Society, London, Special Publications, pp. 85–94.

Trincardi, F., Field, M.E., 1991. Geometry, lateral variation and preservation of downlapping regressive shelf deposits: Eastern Tyrrhenian Sea margin, Italy. J. Sediment. Petrol. 61, 775–790.

Valente, A., Magliuolo, P., Russo, F., 2017. The Coastal Landscape of Cilento (Southern Italy): a challenge for protection and tourism valorisation. In: Soldati, M., Marchetti, M. (Eds.), Landscapes and Landforms of Italy. World Geomorphological Landscapes, pp. 409–419. https://doi.org/10.1007/978-3-319-26194-2_35.

Varzi, A.G., Fallati, L., Savini, A., Bracchi, V.A., Bazzicalupo, P., Rosso, A., Sanfilippo, R., Bertolino, M., Muzzupappa, M., Basso, D., 2023. Geomorphology of coralligenous reefs offshore southeastern Sicily (Ionian Sea). J. Maps. https://doi.org/10.1080/17445647.2022.2161963.

Walbridge, S., Slocum, N., Pobuda, M., Wright, D.J., 2018. Unified Geomorphological Analysis Workflows with Benthic Terrain Modeler. Geosciences 8, 94. https://doi.org/10.3390/geosciences8030094.

Ximenes Neto, A.R., Pinheiro, L.D., Lima Filho, R.P., Miranda de Medeiros, D.H., de Araújo Farrapeira Neto, C., Oliveira Soares, M., Rossi, S., de Morais, J.O., 2025. Shallow-to-mesophotic geomorphic habitats influenced by a drowned incised valley in the Western Equatorial Atlantic. Geo-Mar. Lett. 45, 30. https://doi.org/10.1007/s00367-025-00817-5.